

## Uptake of atmospheric molecules by ice nanoparticles: Pickup cross sections

J. Lengyel,<sup>1,a)</sup> J. Kočíšek,<sup>1,b)</sup> V. Poterya,<sup>1</sup> A. Pysanenko,<sup>1</sup> P. Svrčková,<sup>1,a)</sup> M. Fárník,<sup>1,c)</sup>  
D. K. Zaouris,<sup>2</sup> and J. Fedor<sup>3,c)</sup>

<sup>1</sup>*J. Heyrovský Institute of Physical Chemistry v.v.i., Academy of Sciences of the Czech Republic, Dolejškova 3,  
18223 Prague, Czech Republic*

<sup>2</sup>*School of Chemistry, University of Bristol, Bristol BS8 1TS, United Kingdom*

<sup>3</sup>*Department of Chemistry, University of Fribourg, Chemin du Musée 9, CH-1700  
Fribourg, Switzerland*

Uptake of several atmospheric molecules on free ice nanoparticles was investigated. Typical examples were chosen: water, methane, NO<sub>x</sub> species (NO, NO<sub>2</sub>), hydrogen halides (HCl, HBr), and volatile organic compounds (CH<sub>3</sub>OH, CH<sub>3</sub>CH<sub>2</sub>OH). The cross sections for pickup of these molecules on ice nanoparticles (H<sub>2</sub>O)<sub>N</sub> with the mean size of  $\bar{N} \approx 260$  (diameter  $\sim 2.3$  nm) were measured in a molecular beam experiment. These cross sections were determined from the cluster beam velocity decrease due to the momentum transfer during the pickup process. For water molecules molecular dynamics simulations were performed to learn the details of the pickup process. The experimental results for water are in good agreement with the simulations. The pickup cross sections of ice particles of several nanometers in diameter can be more than 3 times larger than the geometrical cross sections of these particles. This can have significant consequences in modelling of atmospheric ice nanoparticles, e.g., their growth.

### I. INTRODUCTION

Small ice nanoparticles and aerosols play an important role in physics and chemistry of Earth atmosphere.<sup>1</sup> Perhaps the most important example is the ozone hole above Antarctica: some of the key reactions which lead to the ozone depletion process proceed on ice particles in polar stratospheric clouds (PSCs) as proposed by Solomon *et al.* in 1980s.<sup>2</sup> The physics and chemistry of PSC particles has been investigated in great details ever since and covered by a number of articles and reviews, e.g., Refs. 3–5.

All these processes start with the formation and growth of the nanoparticles via homogeneous or heterogeneous nucleation and uptake of various molecules on the particles. In this study we focus on the uptake processes. The initial steps in the ice particle generation are the collisions of water monomers with small water clusters, which prevail under the conditions where there are many more monomers than clusters.<sup>6</sup> Therefore, we focus especially on the pickup of water molecules by the large water clusters. Besides, the pickup of some other typical atmospheric molecules is investigated. These include methane CH<sub>4</sub> as one of the most influential greenhouse gases; NO<sub>x</sub> species represented by NO and NO<sub>2</sub>; hydrogen halides

HCl and HBr important in the ozone depletion process; and volatile organic compounds (VOCs) represented by methanol CH<sub>3</sub>OH and ethanol CH<sub>3</sub>CH<sub>2</sub>OH.

The atmospheric pure ice nanoparticles and pickup processes can be mimicked in the laboratory with large (H<sub>2</sub>O)<sub>N</sub> clusters in molecular beams. If the beam is passed through a chamber (pickup cell) filled with a particular gas, the molecules can collide with the nanoparticles and stick to the surface. The efficiency of this process is reflected by the *pickup cross section*. Recently, we have examined two methods for determining these cross sections with Ar<sub>N</sub> cluster beams.<sup>7</sup> Our measurements were based on two approaches proposed for determination of the mean cluster size in molecular beams: (i) velocity decrease due to the pickup of molecules by the cluster;<sup>8</sup> (ii) Poisson distribution measurements.<sup>9</sup> We concluded that only the first method yielded the correct and reliable results.<sup>7</sup>

This method utilizes the fact that the mean cluster size  $\bar{N}$  in supersonic expansions is known and can be controlled by the cluster source conditions.<sup>10–13</sup> We determine the cross section from variation of the beam velocity with the pickup pressure as outlined in Sec. II. Since the relation between  $\bar{N}$  and the expansion conditions is well established also for water clusters,<sup>14</sup> the method can be extended also to these atmospherically important species.

In the present paper we determine experimentally the cross sections of the ice nanoparticles with the mean size  $\bar{N} = 260$  for the atmospheric molecules mentioned above. For pickup of water molecules we have also performed molecular dynamics simulations, which allow a detailed insight into the molecular mechanism of the pickup process.

<sup>a)</sup>Also at Department of Physical Chemistry, Institute of Chemical Technology Prague, Technická 5, 16628 Prague 6, Czech Republic.

<sup>b)</sup>Also at Department of Surface and Plasma Science, Faculty of Mathematics and Physics, Charles University, V Holešovičkách, 18000 Prague, Czech Republic.

<sup>c)</sup>Authors to whom correspondence should be addressed. Electronic addresses: michal.farnik@jh-inst.cas.cz and juraj.fedor@unifr.ch.

## II. EXPERIMENT

### A. Experimental setup

The pickup experiment and cluster cross section measurements have been described in detail in our recent publication.<sup>7</sup> Therefore, only a brief account of the method will be given here.

The general and comprehensive description of our complex cluster beam apparatus can be found in Refs. 15 and 16. The water clusters were generated in the source chamber by supersonic expansion of a neat water vapor through a conical nozzle (diameter  $d = 90 \mu\text{m}$ , length 2 mm, and opening angle  $\alpha = 30^\circ$ ). The vapor pressure  $P_0$  was determined by heating the reservoir filled with water to a constant temperature  $T_R$ . The nozzle was heated to somewhat higher temperature  $T_0$  to prevent the water condensation. The size of the clusters was controlled by varying the source conditions and the resulting mean cluster sizes could be determined according to the empirical formulas:<sup>14</sup>

$$\bar{N} = D \cdot \left( \frac{\Gamma^*}{1000} \right)^a, \quad \Gamma^* = \frac{\Gamma}{K_c} = \frac{n_0 \cdot d_e^q \cdot T_0^{q-3}}{K_c}, \quad (1)$$

where parameters  $D = 11.6$ ,  $a = 1.886$ , and  $q = 0.634$  were determined from fitting the measured size distributions of large  $(\text{H}_2\text{O})_N$  clusters.<sup>14</sup> The reduced scaling parameter  $\Gamma^*$  was introduced by Hagena<sup>12</sup> to classify various clustering conditions, and for water clusters this parameter and cluster size distributions were studied in Buck's group.<sup>14</sup> The characteristic constant of the expanding gas  $K_c = (r_c \cdot T_c)^{q-3}$  for water was evaluated from  $r_c = 3.19 \text{ \AA}$  and  $T_c = 5684 \text{ K}$ . The equivalent nozzle diameter  $d_e = \frac{d}{\tan(\alpha/2)}$  was given by  $d = 90 \mu\text{m}$  and opening angle  $\alpha = 30^\circ$ . The water vapor density in the source was calculated from the reservoir temperature  $T_R$  and pressure  $P_0$  as  $n_0 = \frac{P_0}{k_B T_0}$  ( $k_B$  is the Boltzmann constant). The stagnation pressure of  $P_0 = 3.2 \text{ bar}$  and nozzle temperature  $T_0 = 428 \text{ K}$  result in the mean cluster size  $\bar{N} = 260$ . The water cluster size distribution produced in the supersonic expansions has a log-normal character with a width  $\Delta N \approx \bar{N}$  as determined in the previous experiments<sup>14</sup> with our present cluster source.

The cluster beam passed through a skimmer with 1 mm opening before entering the differentially pumped scattering chamber. This chamber served as a pickup cell filled with the gas to dope the clusters with various molecules. The effective capture length was  $L = 170 \text{ mm}$  is limited on the other side by a 5 mm orifice to the next chamber. Thus the chamber length is well defined and a possible error of  $\pm 5\%$  due to the gas streaming out of the orifices and pressure inhomogeneity was included in the evaluation of the cross section error bars.

The pressure in the chamber was monitored by Bayard-Alpert ionization gauge (Varian type 571). The background pressure in the pickup chamber was  $\leq 1 \times 10^{-6} \text{ mbar}$ , and the pressure with the pickup gas increased up to  $6 \times 10^{-4} \text{ mbar}$ . The measured pressures for various gasses were divided by the correction factor suggested in the gauge instruction manual. Since the pickup pressure is a critical parameter for the cross section evaluation, great attention was paid to its measurement. The ionization gauge was also calibrated inde-

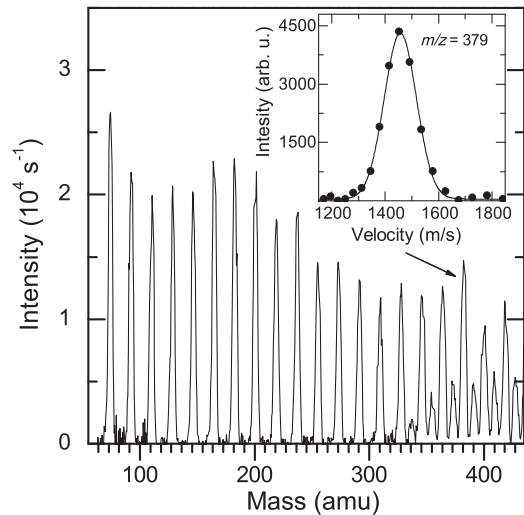


FIG. 1. Fragment ion mass spectrum of  $(\text{H}_2\text{O})_N$   $\bar{N} = 260$  clusters. The inset shows an example of the measured velocity distribution for the  $m/z = 379$  amu mass peak with the Gaussian fit (line).

pendently for the various gases by comparing the measured pressures to the values of a capacitance gauge pressure (Pfeifer CMR 365) and the calibration values were found in good agreement with the values proposed in the instruction manual. The measurements for the various gases were performed repeatedly on different days to avoid any memory effects of the gauge. In each individual measurement, ample time was allowed for stabilization of each pressure step. The cross section measurements for all gases were tested for consistency against a test system (methanol) always before and after each day of measurement. The data for various gases were collected repeatedly over the time period of approximately half a year. The error bars on the measured cross sections include all the effects which appeared to influence the present data.

For the velocity measurements the cluster beam was modulated by a pseudorandom mechanical chopper<sup>17</sup> in the next differentially pumped chamber. The chopper contained two pseudorandom sequences of 127 elements and its rotation with frequency of 492.1 Hz corresponded to a single opening time window of  $8 \mu\text{s}$ . After the chopper the beam passed the flight path of 955 mm through another differentially pumped chamber to the ion source of a quadrupole mass spectrometer with an electron ionizer and channeltron detector. The clusters were ionized with 70 eV electrons. Figure 1 shows an example of the measured fragment mass spectrum. The mass range of our quadrupole mass spectrometer was limited to cluster fragments  $(\text{H}_2\text{O})_k\text{H}^+$  with  $k \leq 25$ . However, Bobbert *et al.*<sup>14</sup> have demonstrated a significant water cluster fragmentation upon electron ionization in direct comparison with Na doping and subsequent photoionization which is essentially fragmentation-free method. Thus also the larger clusters from our size distribution contribute to the present mass peaks, and since the cluster velocity after supersonic expansion is almost independent of their size (within less than 10%), it can be measured on the small fragment mass peaks in the spectrum.

The arrival time to the detector was measured. The total flight time was properly corrected for the time spent by the

ion fragment in the quadrupole and for any electronic delay of the trigger signals and converted to the beam velocity distribution. The velocity distribution was evaluated from the measured data by the cross-correlation mathematical method.<sup>17</sup> The beam velocity was measured for several water cluster fragments and the values were carefully checked for consistency. Typically the velocity dependence on pickup pressure was measured for at least two masses, e.g., on a strong fragment mass peak of  $(\text{H}_2\text{O})_k\text{H}^+$   $k = 10$  at  $m/z = 181$  amu, and at the end of the measured fragment mass range for  $k = 21$  at  $m/z = 379$  amu. The maximum velocity of the water clusters (without any pickup gas) measured at the nozzle temperature  $T_0 = 428$  K was  $v_0 = 1450 \pm 10$  ms<sup>-1</sup>, and the speed-ratio  $S = 2\sqrt{\ln(2)} \frac{v_0}{\Delta_{FWHM} v_0} \approx 17$ . The inset in Fig. 1 shows an example of the measured TOF distribution at the  $m/z = 379$  amu mass peak.

## B. Pickup cross section

We have discussed the pickup cross-section determination in detail in our recent publication.<sup>7</sup> The method is based on the assumption that water clusters in the beam are slowed down by the pickup due to the momentum transfer, and the velocity change increases with the number of guest molecules. Let us assume cluster of a size  $N$  with an initial velocity  $v_i$  colliding with  $k$  stationary molecules in the pickup cell which stick to the cluster. Then the momentum conservation yields for the cluster final velocity  $v_f$  the equation:

$$Nm_C \cdot v_i = (Nm_C + km_X) \cdot v_f, \quad (2)$$

where  $m_C$  is the cluster constituent mass ( $\text{H}_2\text{O}$ ) and  $m_X$  is the mass of the picked-up species.

This formula has two important assumptions: (i) the collision is inelastic, i.e., molecule sticks to the cluster if a considerable momentum transfer between the molecule and the cluster occurs and (ii) no considerable evaporation of cluster occurs upon the pickup. Both assumptions are confirmed for  $\text{H}_2\text{O}$  pickup by molecular dynamics simulations outlined in Sec. IV. The previous investigations<sup>7,8</sup> showed that this simple model described the final velocity dependence very accurately for argon clusters.

The number of picked-up molecules along the path-length  $L$  in a gas at a pressure  $p$  (corresponding to the number density  $n_g = \frac{p}{k_B T}$ ) can be expressed as

$$k = n_g \sigma_e L = \frac{p}{k_B T} \sigma_e L, \quad (3)$$

where  $\sigma_e$  is the pickup cross section. Combining Eqs. (2) and (3), the relative change in the cluster velocity is directly proportional to the pickup cell pressure

$$\frac{\Delta V}{V} \equiv \frac{v_i - v_f}{v_f} = \frac{m_X}{Nm_C} \frac{L \sigma_e}{k_B T} \cdot p. \quad (4)$$

Thus, we plot the relative velocity change as a function of the pressure and fit a linear dependence  $\frac{\Delta V}{V} = \alpha \cdot p$ . From the slope  $\alpha$  the pickup cross section  $\sigma_e$  can be evaluated as

$$\sigma_e = \alpha \cdot \frac{m_C N}{m_X} \cdot \frac{k_B T}{L}. \quad (5)$$

The quantity that is evaluated directly from the experimental data is the effective cross section

$$\sigma_e = \sigma_0 \cdot F_{a0}(\infty, x), \quad (6)$$

which incorporates the velocity-averaging correction factor  $F_{a0}$  due to the velocity distribution of the target molecules.<sup>18-20</sup> Label  $\infty$  denotes the hard sphere potential approximation, and  $x = \frac{v_i}{\alpha_g}$ , where  $v_i$  is the cluster beam velocity and  $\alpha_g$  is the most probable velocity in the Maxwellian distribution of the scattering gas. These correction factors were tabulated in the literature.<sup>18,19</sup>

## III. EXPERIMENTAL RESULTS

Figure 2 shows examples of the measured relative velocity dependencies on the pickup gas pressure  $p$  for several molecules ( $\text{H}_2\text{O}$ ,  $\text{NO}$ ,  $\text{NO}_2$ ) on  $(\text{H}_2\text{O})_N$  clusters  $\bar{N} = 260$ . Such dependencies were measured repeatedly on various days over a long time period to confirm the reproducibility of our data. The figure documents the high quality of the linear fit to the relative velocity change dependence on pickup pressure. A possible source of error in the pickup cross section determination can be the pressure correction factor used for various gases. Therefore, the ion gauge was also calibrated independently with the capacitance gauge, yet the later does not cover the entire measurement pressure range. Thus, the error bars on the pickup cross sections reflect not only the reproducibility of our data which was high, but rather the possible uncertainty in the pressure determination. It ought to be mentioned that the raw data not corrected by the pressure correction factor are shown in Fig. 2.

The measured cross sections are summarized in Fig. 3 and Table I. The geometrical cross section of the water clusters is indicated by the horizontal line. It was evaluated from the water molecule van der Waals radius  $r_w = 1.6$  Å, i.e., the cluster volume corresponds to the volume of  $N$  spheres with  $r_w$  radius multiplied by a factor  $\frac{\sqrt{18}}{\pi}$  accounting for the hexagonal close packing of the hard spheres. Thus, the geometrical cross section was calculated as

$$\sigma_g = \pi R_N^2, \quad R_N = r_w \cdot \left( \frac{\sqrt{18}}{\pi} \cdot N \right)^{1/3}, \quad (7)$$

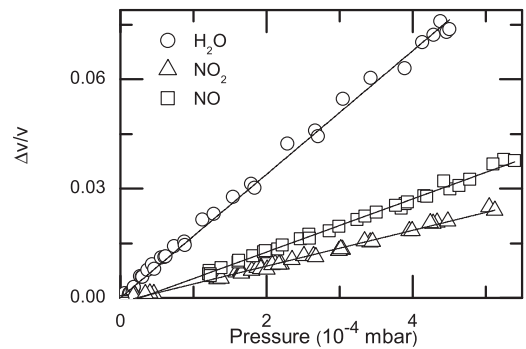


FIG. 2. The relative velocity dependence on the pickup gas pressure  $p$  for  $\text{H}_2\text{O}$  (circles),  $\text{NO}$  (squares), and  $\text{NO}_2$  (triangles) molecules on  $(\text{H}_2\text{O})_N$  clusters  $\bar{N} = 260$  with the linear fits (lines).

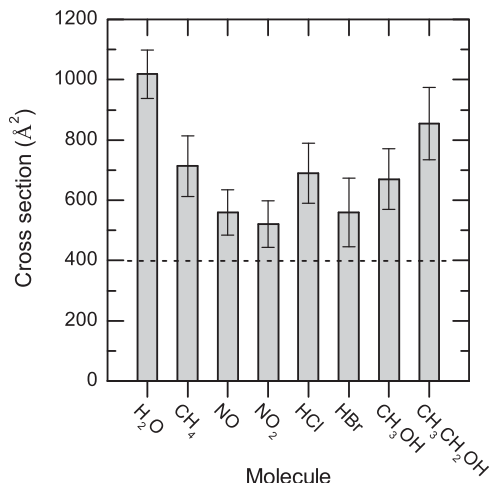


FIG. 3. The pickup cross sections for atmospheric molecules H<sub>2</sub>O, CH<sub>4</sub>, NO, NO<sub>2</sub>, HCl, HBr, CH<sub>3</sub>OH, and CH<sub>3</sub>CH<sub>2</sub>OH on (H<sub>2</sub>O)<sub>N</sub> clusters  $\bar{N} = 260$ . Horizontal line represents the geometrical cross section.

giving the geometrical cross section  $\sigma_g \approx 400 \text{ \AA}^2$  for  $N = 260$ .

#### IV. THEORETICAL CROSS SECTIONS FOR WATER PICKUP

Of the presented experimental cross sections, we focus on the pickup of water molecules, because of its significance for build-up of the ice particles in the initial stages of nucleation. To provide support for the experimental findings, we have performed molecular dynamics (MD) simulations for the (H<sub>2</sub>O)<sub>N</sub>-H<sub>2</sub>O collisions. Simulations provide a value of the cross section that can be compared with the experimental number. Furthermore, by repeating simulations for several cluster sizes, we are able to extend the experimental findings and formulate more general conclusions.

Simulations were done in the coordinate system where the (H<sub>2</sub>O)<sub>N</sub> cluster is initially in rest and the H<sub>2</sub>O molecule is shot at it with the velocity corresponding to experimental cluster beam velocity. In this section we thus call the picked-up molecule a projectile. Each cross section was determined from an ensemble of trajectories with varying impact parameters, where each trajectory was obtained from the MD simulation. The cross section was then evaluated from the maximum impact parameter that leads to the momentum transfer assumed in Eq. (2) used in evaluation of the experimental data. All simulations were done with our own (fortran) code.

The H<sub>2</sub>O-H<sub>2</sub>O interaction was described by the TIP3P model.<sup>21</sup> The model has positive charges on the hydrogens ( $q_H = +0.417e$ ) and negative charge on oxygen ( $q_O = -0.834e$ ). The potential between two water molecules is

a sum of electrostatic Coulomb interaction between all intermolecular pairs and a single Lennard-Jones term between oxygen atoms. The water molecules were not considered rigid, the vibration of intramolecular bonds was treated within harmonic approximation with frequencies matching the experimental frequencies of the normal vibrational modes. This approach is rather unusual—the molecules within the water model are usually kept rigid. We have decided for the present model due to simpler implementation of the trajectory integrating code (no need for a constrain algorithm). Additionally, Zamith *et al.*<sup>22,23</sup> have recently shown that dynamical processes on a short time scale influence sticking properties of charged water clusters. Of course, the explicit treatment of the intramolecular motion brings the necessity of a short numerical time step. For integrating the trajectories, Verlet algorithm with the timestep of 0.2 fs was used. For the largest cluster simulated ( $N = 520$ ) the algorithm conserved the total energy within 0.5% for the simulation length of 20 ps.

The initial cluster structure was obtained by starting with the (H<sub>2</sub>O)<sub>21</sub> cluster with coordinates taken from Cambridge Cluster Database,<sup>24</sup> adding water molecules to this structure one by one and simultaneous cooling of the structure. The whole cluster was heated once more to 300 K and slowly cooled down to 90 K. This was repeated several times and different cluster structures were obtained. The cluster structure obtained this way is certainly not a global minimum of the potential energy surface. As was pointed out in a review by Buch *et al.*,<sup>25</sup> the search for a global energetic minimum in water clusters has plethora of difficulties, including a “rugged energy landscape,” i.e., a multitude of local minima separated by high barriers. However, the quantity investigated here: the calculated pickup cross section is primarily influenced by the long-range interaction between water molecules, thus does not depend on the exact structural conformation of the cluster. This was confirmed by repeating the simulations for several cluster structures. The resulting values of cross section differed by less than 10% for different structures. Moreover, for all cluster sizes, the mean geometrical cross section of the obtained structures (as determined from the radial distribution function from the cluster’s centre of mass) was in very good agreement with the approximative geometrical cross section, Eq. (7).

The simulation of one projectile trajectory proceeded as follows: first the cluster was equilibrated for 5 ps. The cluster temperature was assumed to be 90 K—this was chosen as a compromise between 70 and 100 K as estimated in Ref. 26 for a cluster source identical to ours. Then the cluster was randomly rotated and the H<sub>2</sub>O projectile was shot at the cluster with a certain impact parameter and velocity of 1450 ms<sup>-1</sup>, equal to velocity of cluster beam in the experiment. The whole system was simulated for 20 ps. After the simulation, it was

TABLE I. Cross sections for pickup of several molecules on (H<sub>2</sub>O)<sub>N</sub>,  $\bar{N} = 260$ . The corresponding geometrical cross section is  $\sigma_g \approx 400 \text{ \AA}^2$ , and the simulated cross section for water molecules was  $\sigma_s \approx 946 \text{ \AA}^2$ .

Molecule	H <sub>2</sub> O	CH <sub>4</sub>	NO	NO <sub>2</sub>	HCl	HBr	CH <sub>3</sub> OH	CH <sub>3</sub> CH <sub>2</sub> OH
$\sigma_e(\text{\AA}^2)$	1018 ± 80	713 ± 80	560 ± 75	520 ± 77	690 ± 100	560 ± 114	670 ± 100	855 ± 120

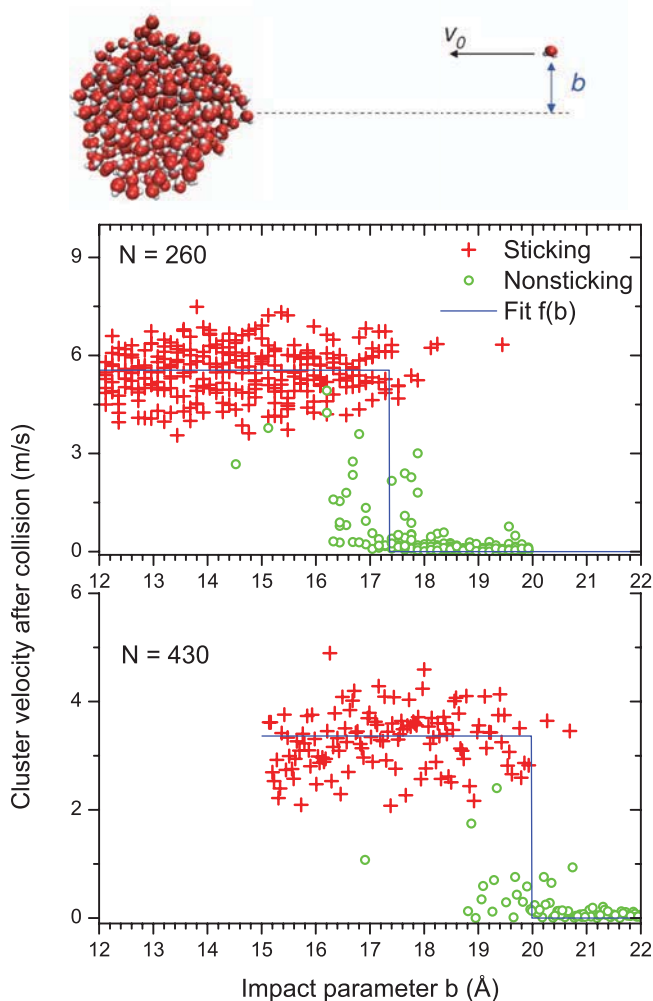


FIG. 4. (Top panel) The MD simulation geometry for one trajectory. (Graphs) The calculated cluster velocity after the collision as a function of the projectile impact parameter. The individual trajectories are categorized as sticking (crosses) or nonsticking (open circles). The line is a fit of the step function  $f(b)$  determining the maximum impact parameter  $b_{max}$ , Eq. (8).

determined whether the collision was sticking or nonsticking and the final cluster velocity was calculated.

In total 250 such trajectories were generated with impact parameter ranging from 12 to 22 Å. The results of simulations: the cluster velocity after the collision vs. the impact parameter of the projectile are plotted in Fig. 4. The momentum transfer follows the expected result: only the sticking trajectories lead to a considerable momentum transfer to the cluster. The data can be approximated by the function (line in Fig. 4)

$$f(b) = v_c [1 - \Theta(b - b_{max})]. \quad (8)$$

Here  $v_c$  is the cluster velocity after collision according to momentum conservation, Eq (2).  $\Theta(x)$  is the Heaviside step function. The maximum impact parameter  $b_{max}$  is determined from one-parameter fit of the function  $f(b)$  to the experimental data. The corresponding cross section is then

$$\sigma = \pi b_{max}^2. \quad (9)$$

The calculated cross section for  $N = 260$  is  $946 \text{ \AA}^2$  which is in good agreement with the experimental value of  $(1018 \pm 80) \text{ \AA}^2$  and it provides support for the experimental finding

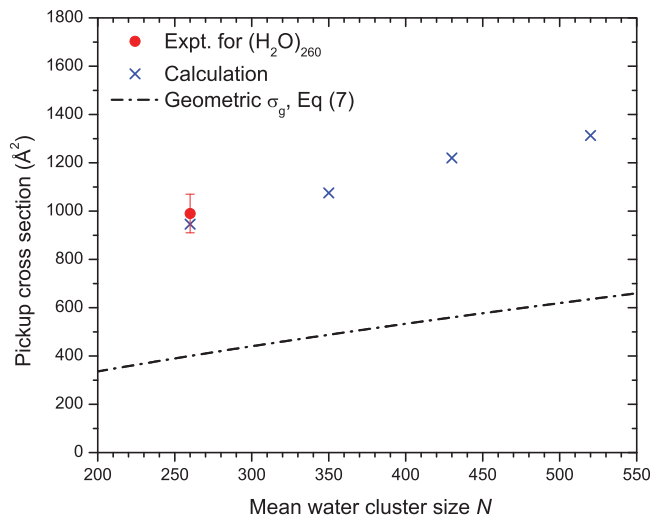


FIG. 5. Cross sections for the pickup of  $\text{H}_2\text{O}$  molecules on  $(\text{H}_2\text{O})_N$ . The full circle is the experimental value for  $\bar{N} = 260$ , the crosses are calculated values for four different sizes of water cluster. The line indicates the corresponding geometrical cross sections calculated from van der Waals radius of  $\text{H}_2\text{O}$ , Eq. (7).

that the pickup cross section is significantly larger than just the geometrical cross section of the cluster. Figure 4 confirms the basic assumption used in evaluating the experimental data [Eq. (2)]—only sticking collisions lead to considerable momentum transfer between the projectile and cluster.

We have repeated the cross section calculation for several cluster sizes,  $\bar{N} = 260, 350, 430, 520$ , in order to observe the general trend. The calculated cross sections are summarized in Fig. 5.

## V. DISCUSSION

The pickup cross sections measured for various molecules on  $(\text{H}_2\text{O})_N$ ,  $\bar{N} \approx 260$  nanoparticles vary between  $520 \text{ \AA}^2$  for  $\text{NO}_2$  and  $1018 \text{ \AA}^2$  for  $\text{H}_2\text{O}$  and are larger than the geometrical cross section of  $400 \text{ \AA}^2$ . We have observed the variation of the pickup cross section for various molecules already previously for argon clusters.<sup>7</sup> The pickup cross section is determined by the strength and extent of the interaction potential between the picked-up molecule and the cluster constituents and also by the mass of the molecule and relative velocity. The later issue is discussed below.

The experimental cross section for the pickup of water molecules ( $1018 \pm 80 \text{ \AA}^2$ ) is within the experimental error in agreement with the value obtained from the molecular dynamics simulations ( $946 \text{ \AA}^2$ ). The measured cross section is by factor of 2.5 larger than the simple geometrical cross section of the nanoparticle. The calculated cross sections for several cluster sizes shown in Fig. 5 suggest that this is a general trend—the calculated values are consistently higher by approximately factor of 2.2. The range of cluster sizes in the graph is not sufficient to see the  $N^{2/3}$  dependence in full extent. The question arises, whether the actual pickup cross section will follow the size dependence of the geometrical cross section. The effect of long-range forces in the cluster-molecule collision has been theoretically investigated by Vasilev and

Reiss,<sup>27,28</sup> for water droplets and by Vigué *et al.*<sup>29</sup> for argon clusters. The later work has shown that the capture cross section for  $\text{Ar}_N$  clusters (which is also larger than the geometrical cross section) scales as  $N^{2/3}$  for  $N \gtrsim 10^3$ . The cluster-molecule potential for water cluster–water molecule interaction is different than the VB potential used by Vigué *et al.* and Fig. 5 suggests, that for water clusters the  $N^{2/3}$  scaling sets on already at the present size range.

An important point which should be discussed is the velocity dependence. The attractive potential between the particle and molecule will pull the slower molecule from a larger distance towards the cluster than the faster one. Thus the pickup cross section will increase with decreasing relative velocity. In the present experiment the cluster velocity is determined by the nozzle temperature which could not be changed significantly enough to observe any effect on the measured cross sections. The cluster velocity corresponds essentially to the relative velocity since it is significantly higher than the thermal velocity of the molecules. The temperature dependence can be estimated from Eq. (6): e.g., for water molecule  $x = \frac{v_i}{\alpha_g} \approx 2.75$  giving  $F_{a0} = 1.066$  (tabulated in Refs. 18 and 19) which yields  $\sigma_0 = 955 \text{ \AA}^2$ . At atmospheric conditions, i.e., in a thermal equilibrium,  $v_i = \alpha_g$  giving  $F_{a0} = 1.47$  and the corresponding effective cross section  $\sigma_e \approx 1400 \text{ \AA}^2$ . This value is larger than the geometrical cross section by factor of 3.5.

Our cross sections can be compared to the attachment cross section of water molecules on mass selected protonated water clusters.<sup>22,23</sup> The experimentally measured cross sections of Zamith *et al.*<sup>22,23</sup> for  $N = 250$  are approximately  $800 \text{ \AA}^2$  (for 33 eV kinetic energy in the lab frame) which is close to our measured and simulated values. Nevertheless the authors report that their cross sections are smaller than the geometrical ones. The major reason for the discrepancy is the different geometrical cross sections reported in the work of Zamith *et al.* compared to our work. We calculate the geometrical cross section according to Eq. (7) considering the water molecule van der Waals radius of  $r_w = 1.6 \text{ \AA}$ . On the other hand Zamith *et al.* derive their geometrical cross section from the molecular radius of  $2.25 \text{ \AA}$ , deduced from the density of bulk ice of about  $2 \text{ \AA}$ . Our simulations suggest that the  $(\text{H}_2\text{O})_N$  cluster structure for  $N = 260$  is far from hexagonal ice lattice structure at least at the temperatures of 90 K considered in our experiments. Besides, it has been also shown by other theoretical calculations<sup>25</sup> that the cluster structures do not correspond to the hexagonal ice lattice structure at least in the mid-size region investigated in our experiments. They assume rather the structure of amorphous solid water, and the cluster radius of 10–13  $\text{ \AA}$ , can be estimated from Fig. 8 in Ref. 25 for the cluster consisting of 293 water molecules which is good agreement with our radius of 11.3  $\text{ \AA}$ , for  $N = 260$  obtained from our Eq. (7) using the van der Waals radius of 1.6  $\text{ \AA}$ . In addition, our simulated cluster diameter (and subsequently its geometrical cross section  $400 \text{ \AA}^2$ ) is also in good agreement with Eq. (7) using the radius of 1.6  $\text{ \AA}$ . This suggests that the geometrical cross section in the work of Zamith *et al.* is overestimated.

The effective integral collision cross sections of small water clusters  $N = 4\text{--}8$  have also been measured by beam

attenuation in various gasses to be  $\sim 100\text{--}300 \text{ \AA}^2$ .<sup>30</sup> However, a direct comparison to the present data is difficult due to the different methods and different evaluated quantities.

The agreement of the measured cross section with the simulated one for water molecules and our previous investigations of Ar-cluster cross sections<sup>7</sup> both suggest high reliability of the present experimental method. The present water cluster cross sections for other molecules range from  $\sigma_e \approx (520 \pm 77) \text{ \AA}^2$  for  $\text{NO}_2$  to  $(855 \pm 120) \text{ \AA}^2$  for ethanol. All the measured values are significantly larger than the geometrical cross sections, and can be expected to be even larger at the thermal equilibrium conditions in the atmosphere in analogy to the above discussion of water molecule pickup.

One possible effect which could lead to overestimation of the observed sticking cross section (essentially by factor of two) would be the head-on elastic collision. The performed MD simulations have not revealed any such events for water molecules where the cross section is the largest one. Besides our previous measurements and simulations of Ar cluster pickup cross sections<sup>7</sup> have not revealed such effect for  $\text{Ar}_n$  which are more rigid compared to the water clusters and the interactions of the molecules with them are much weaker. Despite that we have observed in the simulations mostly sticking collisions—no elastic scattering—and the cross sections were in good agreement with the experiment. Therefore, we conclude that the effects of elastic scattering cannot dominate in the present experiments.

## VI. CONCLUSIONS

We have measured the pickup cross sections of ice nanoparticles for several typical atmospheric molecules in the laboratory experiment with molecular beams. For water molecules the pickup cross sections were also calculated in a molecular dynamics simulation of the pickup process. The agreement between the experimental and calculated cross section values underscores the reliability of our measurements, and the simulations provide detailed insight into the pickup process dynamics.

The measured pickup cross sections for all molecules starting from  $\sigma_e(\text{NO}_2) \approx 520 \text{ \AA}^2$  are larger than the geometrical cross section  $\sigma_g = 400 \text{ \AA}^2$ . The largest measured cross section for water was  $1018 \pm 80 \text{ \AA}^2$ , by factor of 2.5 larger than the geometrical value. The values measured at the beam velocity of  $1450 \text{ ms}^{-1}$  can be extrapolated to the thermal equilibrium atmospheric conditions where the pickup cross sections will be even larger. In particular, for water the corresponding effective cross section will be  $\approx 1400 \text{ \AA}^2$ , i.e., by factor of 3.5 larger than  $\sigma_g$ .

These findings can have consequences in modelling the formation and growth of atmospheric ice nanoparticles. Atmospheric nanoparticle formation consists of a complicated set of processes that include the production of nanometer-size clusters from gaseous vapors, the growth of these clusters to larger sizes, and their simultaneous removal by coagulation with the pre-existing particle population.<sup>31</sup> Considerable effort is devoted to the modelling of initial stages of the particle growth and cluster formation (e.g., Refs. 6 and 32). In these

models, when considering the formation (or evaporation) of clusters, the geometrical cross section of the cluster is used in the expressions for the dynamical rate constants and the collision rates are taken to be hard sphere collision rates. The present data show that the more realistic cross sections should be used instead.

## ACKNOWLEDGMENTS

This work has been supported by the Grant Agency of the Czech Republic Project Nos. 203/090422 and P208/110161 and by the Swiss National Science Foundation Project No. PZ00P2\_1323571. J. Kočíšek and D. Zaouris acknowledge the Grant No. 238671 "ICONIC" within FP7-MC-ITN and D.Z. also acknowledges the support of Professor N. M. R. Ashfold. We gratefully acknowledge discussing our results with Professor U. Buck.

<sup>1</sup>B. J. Finlayson-Pitts and J. J. N. Pitts, *Chemistry of the Upper and Lower Atmosphere* (Academic, San Diego, 2000).

<sup>2</sup>S. Solomon, R. R. Garcia, F. S. Rowland, and D. J. Wuebbles, *Nature (London)* **321**, 755 (1986).

<sup>3</sup>T. Peter, *Ann. Rev. Phys. Chem.* **48**, 785 (1997).

<sup>4</sup>A. J. Prenni and M. A. Tolbert, *Acc. Chem. Res.* **34**, 545 (2001).

<sup>5</sup>A. Bogdan, M. J. Molina, H. Tenhu, E. Mayer, and T. Loerting, *Nat. Chem.* **2**, 197 (2010).

<sup>6</sup>H. Vehkamäki, M. J. McGrath, T. Kurtén, J. Julin, K. E. J. Lehtinen, and M. Kulmala, *J. Chem. Phys.* **136**, 094107 (2012).

<sup>7</sup>J. Fedor, V. Poterya, A. Pysanenko, and M. Fárník, *J. Chem. Phys.* **135**, 104305 (2011).

<sup>8</sup>J. Cuvellier, P. Meynadier, P. de Pujo, O. Sublemontier, J.-P. Visticot, J. Berlande, A. Lallement, and J.-M. Mestdagh, *Z. Phys. D* **21**, 265 (1991).

<sup>9</sup>M. Macler and Y. K. Bae, *J. Phys. Chem. A* **101**, 145 (1997).

<sup>10</sup>O. F. Hagena, *Surf. Sci.* **106**, 101 (1981).

<sup>11</sup>O. F. Hagena, *Z. Phys. D* **4**, 291 (1987).

<sup>12</sup>O. F. Hagena, *Rev. Sci. Instrum.* **63**, 2374 (1992).

<sup>13</sup>U. Buck and R. Krohne, *J. Chem. Phys.* **105**, 5408 (1996).

<sup>14</sup>C. Bobbert, S. Schütte, C. Steinbach, and U. Buck, *Eur. Phys. J. D* **19**, 183 (2002).

<sup>15</sup>R. Baumfalk, U. Buck, C. Frischkorn, S. R. Gandhi, and C. Lauenstein, *Ber. Bunsenges. Phys. Chem.* **101**, 606 (1997).

<sup>16</sup>M. Fárník, *Molecular Dynamics in Free Clusters and Nanoparticles Studied in Molecular Beams* (ICT Press, Prague, 2011).

<sup>17</sup>D. J. Auerbach in *Atomic and Molecular Beam Methods*, edited by G. Scoles (Oxford University Press, New York, Oxford, 1988), Vol. I, p. 362.

<sup>18</sup>K. Berling, R. Belbing, K. Kramer, H. Pauly, C. Schlier, and P. Toschek, *Z. Phys.* **166**, 406 (1962).

<sup>19</sup>N. C. Lang, H. V. Lilienfeld, and J. L. Kinsey, *J. Chem. Phys.* **55**, 3114 (1971).

<sup>20</sup>H. Pauly, *Atom, Molecule and Cluster Beams* (Springer, Berlin, 2000).

<sup>21</sup>W. L. Jorgensen, J. Chandrasekhar, J. D. Madura, R. W. Impey, and M. L. Klein, *J. Chem. Phys.* **79**, 926 (1983).

<sup>22</sup>S. Zamith, P. Feiden, P. Labastie, and J.-M. L'Hermite, *Phys. Rev. Lett.* **104**, 103401 (2010).

<sup>23</sup>S. Zamith, P. Feiden, P. Labastie, and J.-M. L'Hermite, *J. Chem. Phys.* **133**, 154305 (2010).

<sup>24</sup>D. J. Wales, J. P. K. Doye, A. Dullweber, M. P. Hodges, F. Y. Naumkin, F. Calvo, J. Hernández-Rojas, and T. F. Middleton, The Cambridge Cluster Database, see <http://www-wales.ch.cam.ac.uk/CCD.html>.

<sup>25</sup>V. Buch, S. Bauerecker, J. P. Devlin, U. Buck, and J. K. Kazimirski, *Int. Rev. Phys. Chem.* **23**, 375 (2004).

<sup>26</sup>J. Bruderermann, P. Lohbrandt, U. Buck, and V. Buch, *J. Phys. Chem.* **112**, 11038 (2000).

<sup>27</sup>O. V. Vasilev and H. Reiss, *J. Chem. Phys.* **105**, 2946 (1996).

<sup>28</sup>O. V. Vasilev and H. Reiss, *Phys. Rev. E* **54**, 3950 (1996).

<sup>29</sup>J. Vigué, P. Labastie, and F. Calvo, *Eur. Phys. J. D* **8**, 265 (2000).

<sup>30</sup>Z. Sternovsky, M. Horányi, and S. Robertson, *Phys. Rev. A* **64**, 023203 (2001).

<sup>31</sup>M. K. V.-M. Kerminen, *Atmos. Res.* **90**, 132 (2008).

<sup>32</sup>M. Kulmala, *Atmos. Res.* **98**, 201 (2010).